EPR ENLIGHTENING SOME ASPECTS OF PROPANE ODH OVER VO_x- SiO_2 AND VO_x-Al_2O_3

C.Oliva[a]*, S.Cappelli[a], I. Rossetti[a], N.Ballarini[b], F.Cavani[b], L. Forni[a]

[a]*Dip. CFE e ISTM-CNR, Univ. di Milano, via C.Golgi, 19 20133 Milano (Italy)*

Fax: +39 02 50314300. E-mail cesare.oliva@unimi.it

[b]*Dip.Chimica Industriale e dei Materiali, Univ. di Bologna, v.le Risorgimento 4 Bologna*

ABSTRACT

In the oxidative dehydrogenation (ODH) of propane to propylene VO_x–based catalysts prepared by flame pyrolysis (FP) showed more selective than those prepared by impregnation. Furthermore, samples prepared by the same method were less active, but more selective when VO_x was supported on SiO_2 than on Al_2O_3. In order to assess V local structure, V^{4+} ions showed useful labels to characterise these catalysts by EPR spectroscopy. Indeed, the spectrum of a (10 wt%V_2O_5) FP-prepared VO_x/SiO_2 catalyst was typical of isolated, tetragonally distorted, paramagnetic complexes of V^{4+} forming a monolayer on the sample surface with a strong out-of-plane V^{4+} - O bond. In a sample with identical composition, but prepared by impregnation, this bond showed a bit weaker. Furthermore, ferromagnetic domains of clustered V ions formed in the latter sample, hindering at least in part the accessibility to the catalytically active V-based centres. This gives evidence of the higher dispersion of V in the sample bulk provided by the FP preparation method with respect to conventional ones. A by far weaker V^{4+} - O bond was revealed by the EPR spectrum of a (10%V_2O_5) VO_x/Al_2O_3 sample, accounting for its higher oxygen availability, leading to higher activity, but lower selectivity. However, the same catalyst, when prepared by impregnation, showed a ferromagnetic resonance pattern so intense that no EPR spectrum was detectable at all and no information on the V^{4+} - O bond strength was available in that case.

Such semi-quantitative index of the V-O bond strength can be used as an index of oxygen availability, as a tool to assess catalytic activity and selectivity to the desired olefin.

Keywords: EPR; Flame pyrolysis; supported vanadium catalysts; oxidative dehydrogenation of propane.

*) Corresponding author, Fax +39-02-50314300, e-mail: cesare.oliva@unimi.it

1 - **INTRODUCTION**

Oxidative dehydrogenation (ODH) of propane to propylene represents an interesting alternative to the energy demanding dehydrogenation process and supported VO_x demonstrated promising catalysts for this reaction [1-10]. Different supports have been tested, such as ZrO_2 [11,12], TiO_2 [13], V-substituted zeolites or silicalites [14], SiO_2 [7,9,11] and Al_2O_3, usually as the γ- phase [3,4-6,8,10,11,13].

The support plays a key role in this application, since it determines V dispersion as a function of V loading. Indeed, the samples so far described in the literature are commonly prepared by impregnation of the support with a V precursor. Hence, V is dispersed on the surface, accommodating itself as isolated species at low V loading, only. With increasing V loading (or calcination temperature), oligomeric and polymeric species form, leading to larger two-dimensional VO_x domains undergoing redox processes much faster than the monovanadate structures present at lower surface densities. At even higher V loading V_2O_5 segregation occurs, forming three–dimensional V-based structures with inaccessible V-atoms. Therefore, the maximum ODH rate (per V ion) would occur at intermediate V surface densities [1-3]. A monolayer can form at particular V loading (or surface density) depending on the nature of the support. Indeed, at the same vanadia surface density the extent of polymerisation is $Al_2O_3 > ZrO_2 >> SiO_2$ [11]. The support can be also directly involved in the reaction. Indeed, if naked acid sites are present on the support, selectivity to propylene is usually low, due to coke formation. This occurs mainly in the case of alumina- or zirconia-supported samples [3]. In fact, propylene selectivity monotonously increases with increasing V loading until a monolayer is formed, *i.e.* until surface acid sites are covered by the active phase [11]. Furthermore, with alumina-supported samples a mixed $AlVO_4$ phase can form, which is usually reported as not active for the ODH of propane [5].

From the above reported information, it is clear that activity and, most of all, selectivity to propylene strongly depends on how V is dispersed on a properly selected support.

In the recent past our research group set up a method for the preparation of single and mixed nanosized oxides by means of the flame pyrolysis (FP) technique [15-19]. We applied such a synthesis procedure to the preparation of silica- and alumina-supported V samples, which were tested as catalysts for the ODH of propane [20,21]. On the basis of such results, it can be hypothesised that, at least for FP-prepared silica-supported samples, V was more easily inserted into the support matrix, leading to a higher dispersion of the active sites, at difference with samples of similar composition prepared by different techniques. An extensive description of the catalytic performance and physical-chemical properties of these samples has been reported elsewhere [20,21]. In the present investigation we concentrated on their characterisation by Electron Paramagnetic Resonance (EPR), a powerful tool to address the local structure of V^{4+} sites. Indeed, this spectroscopic technique can provide information on metal dispersion and on the strength of the V-O interaction. Some interesting remarks on this topic are here presented in the present paper.

2 - EXPERIMENTAL

2.1 - Sample Preparation

A detailed description of the FP preparation procedure and of the effect of the main operating parameters on catalyst properties can be found elsewhere [15-18]. Briefly, a proper amount of precursor salts were dissolved in an organic solvent (alcohol, carboxylic acid or a mixture of them), so to obtain a 0.1-0.2 M solution (concentration referred to the nominal oxide composition). This solution (4.4 cm^3/min), together with 5 L/min of oxygen

(SIAD, purity >99.95%), was fed to the burner. The cross section area of the burner nozzle was adjusted so to have a pressure drop of 0.4 bar across the nozzle. The catalyst powder so produced was collected by means of a 10 kV electrostatic precipitator [15,19].

The feeding solutions have been prepared as described in [20,21], using $Al(NO_3)_3*9H_2O$, tetra-ethyl-orthosilicate (TEOS) and V oxi-acetyl-acetonate as precursors. The solvent consisted of a 1:1 (vol/vol) mixture of ethanol and 1-octanol for the alumina based samples, whereas 1:1 (vol/vol) mixture of ethanol and propionic acid was employed for the silica based ones.

The composition of the samples prepared is reported in Table 1.

2.2 – *Sample Characterisation*

Specific surface area has been determined by N_2 adsorption/desorption at 77K on a Micromeritics ASAP2010 instrument (Table 1). XRD analysis (Fig.1) was carried out on a Philips PW3020 powder diffractometer, by using the Ni-filtered Cu Kα radiation (λ=1.5148 Å). The diffractograms obtained were compared with literature data for phase recognition [22]. Scanning electron microscopy (LEICA, LEO1430) was used to investigate particle morphology.

Electron paramagnetic resonance (EPR) spectra were collected by a Bruker Elexsys instrument, equipped with a standard rectangular ER4102ST cavity and operating at X band, 6.36 mW microwave power and 100 kHz Gauss modulating amplitude. The detection temperature was regulated in the range between 120 and 300 K by gaseous N_2 flowing through liquid Nitrogen and controlled by the Bruker ER4111VT unit . The intensity of the magnetic field was carefully checked by a Bruker ER35M teslameter and the microwave frequency was measured by a HP 5340A frequency meter. Spectral simulations were done by means of the Bruker SimFonia programme.

In any EPR measurement, the same amount of catalyst powder was put in a standard quartz sample holder fulfilling the (25 mm long and 2mm large) sensitive portion of the TE_{102} microwave resonating cavity. This let us to obtain the highest filling factor and therefore the highest signal-to-noise ratio, in all the EPR spectra [23].

The V(IV) concentration was evaluated by comparing the double integral of the EPR spectrum with that of the “strong pitch” appositely provided by Bruker Biospin GMBH, and characterized by a certified “spin concentration” of 3.67 10^{15} spins/cm of sample length.

2.3 – *Catalytic activity tests*

Catalytic activity was measured by means of a continuous, quartz tubular reactor (i.d.= 7 mm) heated by a furnace. The catalyst (0.90 mL, 0.5-0.6 g, 0.425-to-0.600 mm particle size) was activated prior to each run in 20 cm^3/min flowing air, while increasing temperature by 10°C/min up to 550°C, then kept for 1 h. The flow rate of the reactants mixture for the “co-feeding mode” test was 11 cm^3/min of C_3H_8 (20 mol%) + 11 cm^3/min of O_2 (20 mol%) + 28 cm^3/min of He + 4 cm^3/min of N_2 (60 mol% inert). For the “anaerobic mode” flow rates were 6 cm^3/min of C_3H_8 (22 mol%) + 19 cm^3/min of He + 2 cm^3/min of N_2. Contact time was 1 s for the former and 2 s for the latter testing mode, respectively. The exit gas was analysed by means of a micro-GC (Agilent 3000A), equipped with a TCD detector, Plot-Q, OV-1 and MS-5A columns for a complete detection of the effluent products. In addition to propane, propylene, CO and CO_2, the products also include H_2, light alkanes and alkenes, acetic and acrylic acid, detected by using He as carrier gas.

The catalyst was diluted with inert steatite particles and bed temperature was measured by means of an axial thermocouple inserted inside it. During co-feed mode tests, the maximum temperature difference in the axial direction was 7°C. For redox-decoupling tests (anaerobic mode), the temperature profile was more uniform during both

the reduction and the re-oxidation steps, the maximum T gradient along the catalyst bed being around 4-5°C.

During the cyclic mode of operation, the feed containing diluted propane was fed over the catalyst pre-activated with air for a period of 30 minutes, with instantaneous sampling of the effluent stream every 5 minutes. The first sampling was made after 0.5 min from the beginning of the reduction period, which corresponds to the reactivity of the oxidized catalyst. During the reoxidation step, air was fed for 30 minutes, sufficient to completely recover the initial oxidation state, according to preliminary tests.

3 - RESULTS

The EPR spectral profile was independent of the concentration of VO_x on SiO_2, whereas the spectral intensity increased with V concentration, as well as with decreasing sample temperature, as it is foreseen by the Curie-Weiss law. The EPR pattern obtained with the 10%V_2O_5 FP-prepared (V10Si) sample (Fig.2, bottom) is compared with that of a sample with the same chemical composition but prepared by the traditional impregnation method (V10Si-i sample) (Fig.2, top). The latter is composed of at least two FMR' and FMR" Ferromagnetic Resonance bands centred at *ca.* 250 and 3391 G, respectively, and with intensity slightly increasing with decreasing temperature. In addition, a Paramagnetic Resonance spectrum (P') was also detected, but only when analysing the sample at low temperature. P' was rather similar to the P spectrum obtained with the V10Si-V50Si samples and evidenced in Fig.2 (bottom). The same P contribution is also reported in detail in Fig.3 (dotted track), where it is compared to the EPR spectrum obtained with sample V10Al (Fig.3, thicker line). Figure 3 evidences that the EPR line widths were always broader with Al_2O_3- than with SiO_2-supported samples. The EPR spectrum was also *ca.* three times more intense for V10Al than for V10Si. Analogous considerations hold with increasing V content, *e.g.* by comparing FP-prepared V25Al and V25Si samples

(Fig.4). In the last figure, an intense ferromagnetic band (FMR) is also evident in the spectrum of the V25Al sample. At even higher V concentration the ferromagnetic contribution completely overcame any EPR spectrum in the case of Al_2O_3 supported catalysts.

A summary of the results obtained under anaerobic reaction conditions is reported in Table 2. More detailed data have been reported elsewhere [20-21]. For both the preparation methods the conversion was lower, but the selectivity was higher with SiO_2- than with Al_2O_3-supported catalysts. In addition, with the same support, the FP-prepared samples were more selective than those prepared by impregnation (Table 2). This is particularly evident with the SiO_2-based catalysts. Indeed, the propylene yields of the differently prepared alumina-based samples were similar, though also in this case conversion was lower and selectivity higher with the FP-sample than with the catalyst prepared by impregnation (Table 2).

A lower conversion was always obtained with SiO_2- than with Al_2O_3-supported catalysts in the co-feed mode (Fig.5) This corresponded to a higher selectivity to propylene at temperatures between *ca.* 350 and 400°C (Fig.6). The overall performance was roughly similar for the alumina-based samples prepared by the two (FP and impregnation) methods, differences arising only when SiO_2 was used as support.

4. DISCUSSION

The FP preparation of V-based catalysts supported on silica or alumina has been recently described by our group [20,21] as a mean to obtain nanosized catalysts with relatively high surface area. The latter parameter showed strongly dependent on the support nature (around 20 m^2/g for Al_2O_3 and 40-80 m^2/g for SiO_2, depending on V loading) and ultimately related to the preparation protocol. Lower surface area was indeed

achieved during the preparation of the alumina supported samples due to the need of dissolving the aluminum precursor in alcohols, which usually lead to worse powder properties [17,18,21].

XRD patterns of silica supported samples were typical of amorphous materials. At high V loading broad reflections of V_2O_5 appeared. The same reflections were always present for V-Al_2O_3 samples, even at low V loading, together with peaks at $2\theta \approx 45°$ and 68°, due to δ- or η- Al_2O_3 [22]. Anyway, reflections broadening was evident due to nanostructuring. The latter feature was confirmed by SEM analysis, showing mean particle size lower than 100 nm. The particles of silica-based samples did not show a well defined morphology, while alumina supported ones were approximately spherical, but characterized by less uniform size distribution. V_2O_5 segregation in XRD patterns at high loading and with alumina supported samples is in line with the results of FT-IR and Raman analysis on both the catalytic systems [20,21]. On this basis it is possible to conclude that better V dispersion has been achieved with the silica-based catalysts than with the alumina-based ones.

The catalytic activity of the FP-prepared alumina-supported samples was similar to that of a reference catalyst prepared by impregnation when tested under aerobic reaction conditions (co-feed mode). By contrast, the FP-prepared silica-based sample displayed higher conversion and selectivity with respect to its homologue prepared by impregnation. The difference brought about by the two preparation methods became by far more evident when comparing the performance under anaerobic conditions (alternate feed). Indeed, the alumina based samples showed higher conversion and lower selectivity with respect to the silica based ones. Nevertheless, the FP-prepared V10Si sample was by far more selective than the reference V10Si-i sample prepared by impregnation.

In order to better understand the catalyst behavior under such conditions it is important to understand the extent of oxygen availability, related also to the distribution of

the active centres on the surface of the oxidised catalyst. At this aim, the EPR analysis can provide useful information. Indeed, this technique is sensitive to the formation of ferromagnetic clusters of V^{4+}, as revealed by the ferromagnetic patterns of Fig.2 for a sample supported on SiO_2 prepared by impregnation. The fact that samples obtained by the latter procedure are always less selective than those prepared by FP can be explained by a less homogeneous V dispersion occurring in the former and leading to an easier clustering of the paramagnetic centers into ferromagnetic (FM) domains on their surface. These systems form also with FP-prepared samples supported on Al_2O_3 but at high V loading only (Fig.4). On the other hand, the EPR evidence of these ferromagnetic centers can be a possible tool to assess V dispersion. Of course this can be helpful to interpret catalytic activity, since lower dispersion and V_2O_5 segregation lead to lower accessibility to isolated V active sites, ending in progressively lower propylene yield (Table 2).

The FM domains form when the vanadium deposition occurs exclusively on sample surface, without incorporation in the support matrix. These clusters can be related to the presence of three dimensional VO_x crystallites. Their presence in the here reported EPR spectra is in line with XRD data, indicating V_2O_5 segregation, and with previously reported results on the same samples obtained by and FT-IR and Raman [20,21].

Samples characterised by an extensive VO_x segregation show indeed poorer catalytic properties for the ODH reaction, with very low propylene selectivity. This observation is in line with literature data [1]. For example, only 40% of active sites were available for catalytic turnover of the V10Al-i sample prepared by impregnation.

Furthermore, EPR analysis can be a valuable help also because it is sensitive to V^{4+} local structure and it allows a quantification of V-O bond strength. Indeed, though according to literature data [2] V^{4+} concentration is usually low with respect to the total V amount, in any case it is involved in the catalytic process, because the solid would provide active oxygen due the $V^{5+} \leftrightarrow V^{4+}$ (Step I) and/or to the $V^{4+} \leftrightarrow V^{3+}$ (Step II) transition. A

prevailing of the former reduction mechanism would imply a more intense EPR spectrum after the reaction, the opposite holding when reduction occurs down to V^{3+}. The reverse reactions take place during the reoxidation step of the reaction, according to a Mars van Krevelen mechanism. The high-resolution EPR spectra obtained with SiO_2-supported FP samples allows to evaluate [24] the amount of the EPR-sensitive V^{4+} ions present in those samples. That amount was *ca.* 2 mol% V^{4+} with respect to total V amount for V10Si and progressively decreased down to *ca.* 0.4 mol% with increasing V loading up to 50 wt%. This is in line with the observed segregation of V as V_2O_5 (Fig.1).

A (Gaussian) EPR line width of *ca*. 50 G was reported in literature [25] both with Al_2O_3 and SiO_2 as supports for V_2O_5 and attributed to inhomogeneous broadening due to static disorder. On the contrary, the EPR lines were always Lorentzian-shaped with our samples. Therefore, homogeneous rather than inhomogeneous line broadening would be present in them. A line-width value close to 60 G as in [25] has been found only in the case of VO_x/Al_2O_3, whereas *ca*. 15 G narrow lines were recorded with VO_x/SiO_2. This means that the V^{4+} ions are closer to each other in the former samples, causing line broadening through spin-spin interactions. This confirms the lower V-dispersion with alumina-supported catalysts with respect to silica-based ones. Therefore, in the latter case X = V might be supposed in the paramagnetic centres of Fig.7.

The actual location of V^{4+} ions in host lattices has been the subject of many controversial debates in V^{4+} doping $ZrSiO_4$ [26-32] or supported on Al_2O_3, SiO_2, etc. [25,33,34]. In some cases the EPR spectra were detected with V_2O_5/γ-Al_2O_3 only at low temperature, leading [33] to the hypothesis that V^{4+} was localized in distorted octahedrons or tetrahedrons of surrounding oxygen atoms affected by dynamic Jahn-Teller exchange. However, in other cases [25,34] the EPR spectra were detectable at least up to room temperature and were characterised by $g_{//} < g_{\perp}$, as in the present investigation (Fig.3),

where $g_{//}$ and $g_{\perp}$ are the parameters characterising the Zeeman energy of the paramagnetic ion when the external magnetic field is parallel or perpendicular to the V-O axis, respectively [35,36]. These EPR spectra were attributed to surface V^{4+}-based species with a V-O bond perpendicular to the sample surface. In all these cases, the $g_{//} < g_{\perp}$ values were attributed to tetragonal distortion. The electron energy levels of the unpaired $3d^1$ electron in tetragonally distorted octahedron are as shown in Fig.8 [35,36]. The $g_{//}$ values of Fig.3, identical for the two compared spectra, indicate identical Δ_2 energy separation between $d_{x^2-y^2}$ and d_{xy} levels for the FP-prepared catalysts supported on SiO_2 and on Al_2O_3. By contrast, a higher $g_{\perp}$ value of V^{4+} is observed for VO_x supported on SiO_2 than on Al_2O_3 (Fig.3). This indicates that the separation Δ_1 between d_{xz} and d_{yz} and the fundamental d_{xy} levels of V^{4+} is about 2.4 times higher with the former than with the latter support. This ratio is nearly the same with SiO_2 samples prepared by FP and by impregnation, though in the latter case a bit different value of $g_{//}$ has been found [20].

Furthermore, it has been shown [25] that an increased value of the parameter:

$$B = (g_{//} - g_e) / (g_{\perp} - g_e) \qquad (1)$$

indicates a shortening of the out-of-plane V-O bond or an increased distance of the oxygen ligands in the basal plane, g_e being the Zeeman energy parameter of the free electron. In any case, both these situations are index of a strengthening of the V-O interaction [25]. The values B = 1.47 for alumina-supported FP sample and B = 3.60 and 3.50 for silica-supported samples prepared by FP and by impregnation, respectively, have been reported elsewhere [20,21]. These results further support the above considerations and are in line with the literature results [25] always reporting B(Al) < B(Si) values.

Higher B values, *i.e*. stronger V - O bonds, are known for more selective catalysts for methanol oxidation to formaldehyde [25]. However, the same parameter was associated to lower catalytic conversion in an oxidation reaction, as reported in [34] for vanadium mixed oxides.

Therefore, on this basis a higher conversion is expected for the present VO_x/Al_2O_3 than for VO_x/SiO_2, though the latter would lead to a higher selectivity. This hypothesis, based on EPR data only, is perfectly in agreement with activity data under anaerobic conditions reported in Table 2. For samples prepared with the same procedure, the selectivity to propylene was higher for silica supported samples than for the alumina-based ones and the opposite stands for conversion.

The above reported considerations bring to the conclusion that EPR analysis allows to compare the strength of the V^{4+}-O interaction for different catalytic systems, stronger interactions always corresponding to lower conversions and higher selectivity, especially under anaerobic reaction conditions.

A good matching of the EPR-derived previsions on catalytic performance was observed also for the co-feeding mode. Indeed, a higher conversion is obtained for VO_x/Al_2O_3 than for VO_x/SiO_2 samples (Fig.5), whereas the latter lead to a higher selectivity at least at temperatures not higher than *ca*. 550°C where direct dehydrogenation of the paraffin can intervene (Fig.6).

At last, our catalysts have been analysed by EPR also after use. Spectral intensity always decreased after operation under co-feed conditions. By contrast, V^{4+} concentration increased after testing in anaerobic mode. Taking as example sample V28Si, its spectral intensity increased by *ca*. 4 times after use under anaerobic mode, corresponding to *ca*. 3 mol% of V^{4+} ions with respect to the total V amount. From the present results it is hard to assess how V^{4+} participates to the reaction in oxidising atmosphere. Indeed, it is not possible to assess if V^{4+} oxidizes to V^{5+} or reduces to V^{3+}, being likely involved in the redox cycle described by the above mentioned Mars van Krevelen mechanism. However, when considering the used samples after anaerobic activity testing, it is possible to conclude that V^{4+} is one of the products of catalyst reduction. This is much more evident for alumina supported samples than for silica-based ones. Indeed, the spectra of the latter only

increased in intensity, whereas the former transformed into a lorentzian-shaped spectrum [20,21]. This means that a higher amount of V^{4+} ions form with alumina supported samples, intimately interacting with each other with orbitals overlapping, causing an exchange narrowed EPR pattern.

Conclusions

The EPR analysis, though sensitive to the V^{4+} sites only, showed a powerful tool to elucidate the local structure of the active sites and their affinity towards oxygen in an indirect way. This can allow to draw reliable previsions on the performance of the V-based catalysts. Furthermore, this technique allowed to evidence V segregation due to the formation of clustered ferromagnetic domains. This phenomenon can be again correlated to catalytic activity and to selectivity to propylene, the former property increasing, the latter decreasing with increasing the contribution of segregated V.

References

1. M.D. Argyle, K. Chen, C. Resini, C. Krebs, A.T. Bell, E. Iglesia, J. Phys. Chem. B 108 (2004) 2345.
2. N. Steinfeldt, D. Müller, H. Berndt, Appl. Catal. A Gen. 272 (2004) 201.
3. T. Blasco, A. Galli, J.M. Lòpez Nieto, F. Trifirò, J. Catal. 169 (1997) 203.
4. A. Bottino, G. Capannelli, A. Comite, S. Storace, R. Di Felice, Chem. Eng. J. 94 (2003) 11.
5. E.V. Kondratenko, N. Steinfeldt, M. Baerns, Phys. Chem. Chem. Phys. 8 (2006) 1624.
6. M.D. Argyle, K. Chen, A.T. Bell, E. Iglesia, J. Catal. 208 (2002) 139.
7. Z. Zhao, Y. Yamada, A. Ueda, H. Sakurai, T. Kobayashi, Catal. Today 93–95 (2004) 163.
8. M.V. Martìnez-Huerta, X. Gao, H. Tian, I.E. Wachs, J.L.G. Fierro, M.A. Bañares, Catal. Today 118 (2006) 279.
9. N. Ballarini, A. Battisti, F. Cavani, A. Cericola, C. Lucarelli, S. Racioppi, P. Arpentinier, Catal. Today 116 (2006) 313.
10. N. Ballarini, F. Cavani, A. Cericola, C. Cortelli, M. Ferrari, F. Trifirò, G. Capannelli, A. Comite, R. Catani, U. Cornaro, Catal. Today 91–92 (2004) 99.
11. H. Tian, E.I. Ross, I.E. Wachs, J. Phys. Chem. B 110 (19) (2006) 9593.
12. K. Chen, E. Iglesia, A.T. Bell, J. Catal. 192 (2000) 197.
13. D. Shee, T.V. Malleswara Rao, G. Deo, Catal. Today 118 (2006) 288.
14. S. Dzwigaj, I. Gressel, B. Grzybowska, K. Samson, Catal. Today 114 (2006) 237.
15. G.L. Chiarello, I. Rossetti, L. Forni, J. Catal. 236 (2005) 251.
16. G.L. Chiarello, I. Rossetti, P. Lopinto, G. Migliavacca, L. Forni, Catal. Today 117 (2006) 549.
17. G.L. Chiarello, I. Rossetti, L. Forni, P. Lopinto, G. Migliavacca, Appl. Catal. B Environ. 72 (2007) 218.
18. G.L. Chiarello, I. Rossetti, L. Forni, P. Lopinto, G. Migliavacca, Appl. Catal. B Environ. 72 (2007) 227.
19. R.A.M. Giacomuzzi, M. Portinari, I. Rossetti, L. Forni, in: A. Corma, F.V. Melo, S. Mendioroz, J.L.G. Fierro (Eds.), Studies Surface Science and Catalysis, vol. 130, Elsevier, Amsterdam, 2000, p. 197.
20. I. Rossetti, L. Fabbrini, N. Ballarini, C. Oliva, F. Cavani, A. Cericola, B. Bonelli, M. Piumetti, E. Garrone, H. Dyrbeck, E.A. Blekkan, L. Forni, J. Catal., 256 (2008) 45.
21. I. Rossetti, L. Fabbrini, N. Ballarini, C. Oliva, F. Cavani, A. Cericola, B. Bonelli, M. Piumetti, E. Garrone, H. Dyrbeck, E.A. Blekkan, L. Forni, Catal. Today, 141 (2009) 271.
22. Advanced Selected Powder Diffraction Data, Miner. DBM (1–40), J.C.P.D.S., Swarthmore, PA, 1974–1992.
23. R.S. Alger, “Electron Paramagnetic Resonance: Techniques and Applications”, John Wiley Interscience Publ., 1968.
24. G. Catana, R.R. Rao, B.M. Weckhuysen, P. Van Der Voort, E. Vansant, R.A. Schoonheydt, J. Phys. Chem. B, 102 (1998) 8005.
25. V.K. Sharma, A. Wokaun and A. Baiker, J. Phys. Chem., 90 (1986) 2715.
26. T. Demiray, D.K. Nath, F.A. Hummel, J. Am. Ceram. Soc., 53 (1970) 1.
27. D. de Waal, A.M. Heyns, G. Pretorius, R.J.H. Clark, J. Raman Spectr., 27 (1996) 657.
28. H. Xiayou, B. Gui-Ku, Z. Min-Guang, J. Phys. Chem. Solids, 46 (1985) 719.
29. P. Chandley, R.J.H. Clark, R.J. Angel, G.D. Price, J. Chem. Soc., Dalton Trans., 9 (1992) 1579.

30. M. Ocana, A.R. Gonzalez-Elipe, V.M. Orera, P. Tartaj, C.J.Serna, R.I.Merino, J. Am. Ceram. Soc., 81 (1998) 395.
31. A. Siggel, M. Jansen, Z. Anorg. Allg. Chem., 583 (1990) 67.
32. A. Niesert, M. Hanrath, A. Siggel, M. Jansen, K. Langer, J. Solid State Chem., 169 (2002) 6.
33. K.V.R. Chary, B. Mahipal Reddy, N.K. Nag, V.S. Subrahmanyam, J. Phys. Chem., , 88 (1984) 2622.
34. A. Gervasini, G. Fornasari, G. Bellussi, Applied Catalysis A: General, 83 (1992) 235.
35. J.E. Wertz, J.R. Bolton, “Electron Spin Resonance. Theory and Applications”, McGraw–Hill, New York, 1972, 288.
36. N.M. Atherton, “Principles of Electron Spin Resonance”, Ellis Horwood PTR Prentice Hall, 1993.

Table 1: Catalysts composition and surface area (SSA_{BET}).

Sample	nominal %V_2O_5	Support	Preparation method	SSA_{BET} (m^2/g)
V10Si	**10**	**SiO_2**	**Flame Pyrolysis**	**75**
V10Si-i	**10**	**SiO_2**	**Impregnation**	**/**
V28Si	**25**	**SiO_2**	**Flame Pyrolysis**	**80**
V50Si	**50**	**SiO_2**	**Flame Pyrolysis**	**46**
V10Al	**10**	**Al_2O_3**	**Flame Pyrolysis**	**19**
V25Al	**25**	**Al_2O_3**	**Flame Pyrolysis**	**23**
V50Al	**50**	**Al_2O_3**	**Flame Pyrolysis**	**27**
V10Al-i	**10**	**Al_2O_3**	**Impregnation**	**20**

Table 2: Initial conversion, propylene selectivity and yield (referring to the oxidised catalyst) at different temperature under alternate feed.

Sample	Reaction temperature (°C)	Conversion %	Propylene Selectivity %	Propylene yield %
V10Al	410	5.5	53.6	2.9
	500	14.8	43.8	6.5
	550	16.9	54.4	9.2
V10Al-i	450	5.4	55.0	3.0
	500	15.2	40.1	6.1
	550	23.8	38.4	9.1
V10Si	500	10.1	46.2	4.7
	550	14.0	76.4	10.7
V10Si-i	500	9.3	37.8	3.5
	550	16.4	44.7	7.3
V28Si	450	13.0	14.7	1.9
	500	29.0	17.1	4.9
	550	30.5	33.5	10.2
V50Si	450	8.2	19.4	1.6
	500	38.0	3.1	1.2
	550	49.2	2.4	1.2

Captions of Figures

Fig.1 XRD patterns of some representative samples.

Fig.2 EPR spectra of the 10%V_2O_5 sample supported on SiO_2. Preparation by impregnation (top) and by Flame Pyrolysis (bottom). The former pattern, recorded at 118 K, is composed of two ferromagnetic contributions FMR' and FMR" to which a paramagnetic pattern P' adds. The last is detectable at low temperature only and is similar to the paramagnetic spectrum P which is obtained with the sample prepared by Flame Pyrolysis.

Fig.3 The P spectrum of Fig.1 (10%V_2O_5 FP-prepared on SiO_2) is here reported (dotted pattern, spectral intensity x 2.5) for comparison with V10Al. The interpretation scheme is partially shown. The thinner lines refer to the former, the thicker to the latter spectrum.

Fig.4 EPR spectra obtained with *ca.* 25%V_2O_5 supported on Al_2O_3 (top) and on SiO_2 (bottom) (FP-prepared samples). In the former spectrum a broad and intense FMR band appears. The intensity of the latter spectrum has been multiplied x3 for graphical reasons.

Fig.5 Conversion (mol%) *vs*. T obtained with 10%V_2O_5 supported on (♦;◊) SiO_2 and on (▲;Δ) Al_2O_3. Samples prepared by FP method (full symbols) and by impregnation (empty symbols). Reaction carried on in the co-feed mode.

Fig.6 Selectivity to propylene *vs*. T obtained with 10%V_2O_5 supported on (♦;◊) SiO_2 and on (▲;Δ) Al_2O_3. Samples prepared by FP method (full symbols) and by impregnation (empty symbols). Reaction carried on in the co-feed mode.

Fig.7 Catalytic active centres before (up) and after (bottom) the first step of the ODH reaction. The up-right sketch fits well with the high dispersion achieved with the SiO_2 supported samples.

Fig.8 The electron level of a d^1 ion like V^{4+} in tetragonally compressed octahedral crystal field and its relation with the EPR $g_{//}$ and $g_{\perp}$ spectral parameters.

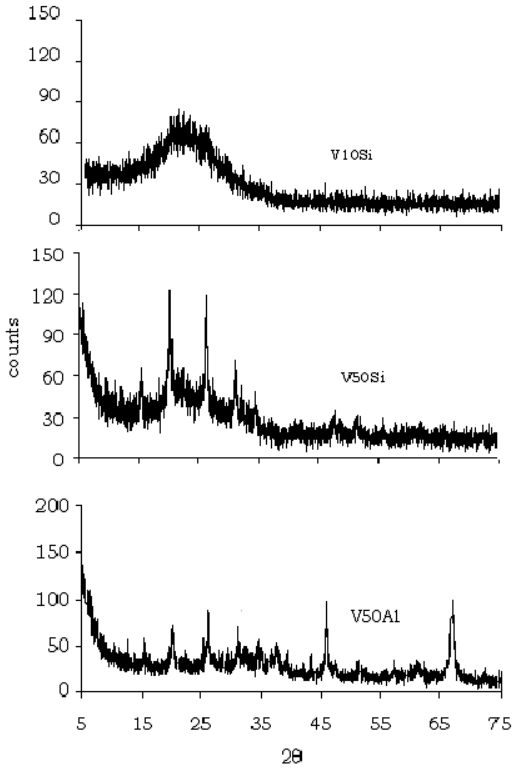
150
120
90
60
30
0
V10Si
150
120
90
60
30
0
counts
V50Si
200
150
100
50
0
V50Al
5
15
25
35
45
55
65
75
2θ

Fig.1

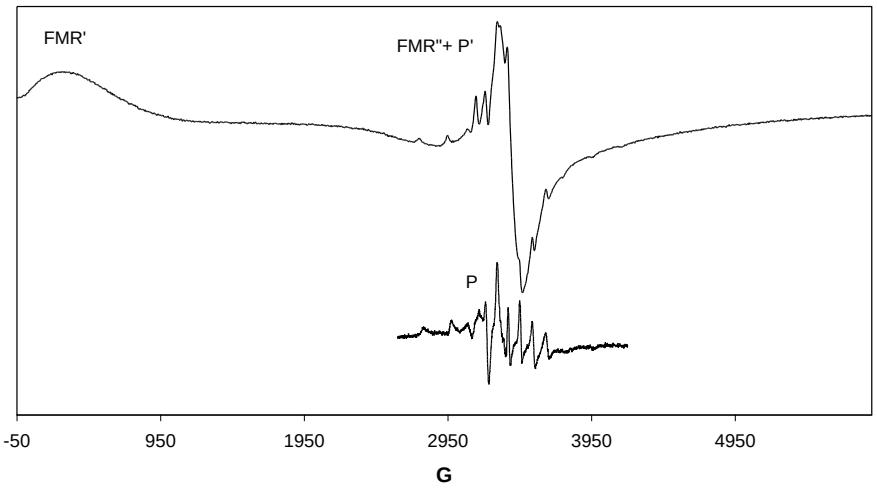
FMR'
FMR"+ P'
P
-50
950
1950
2950
3950
4950
G

Fig.2

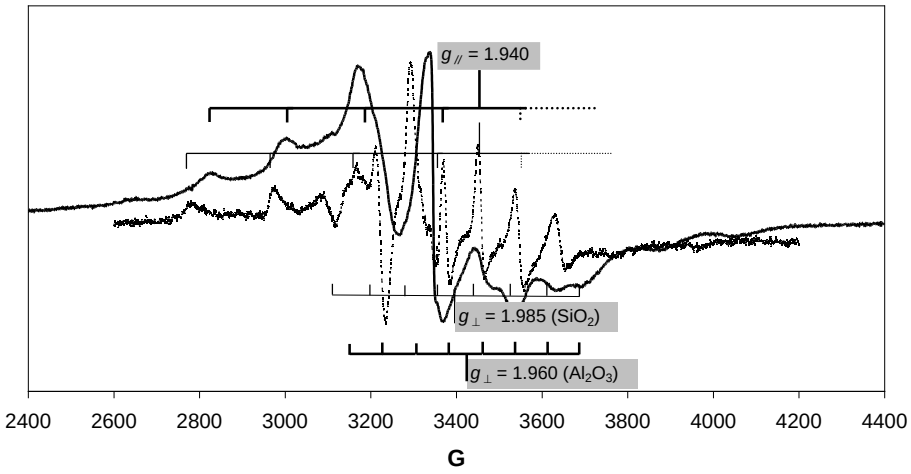

Fig.3

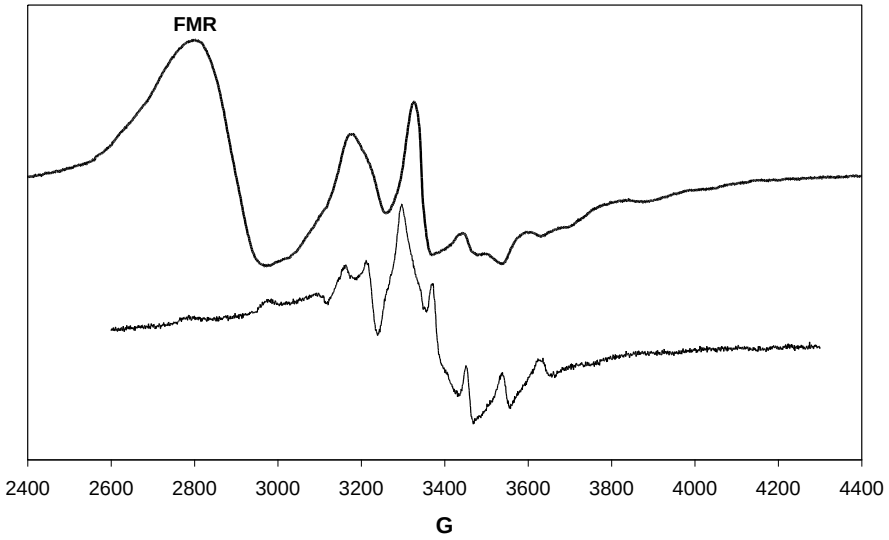

Fig.4

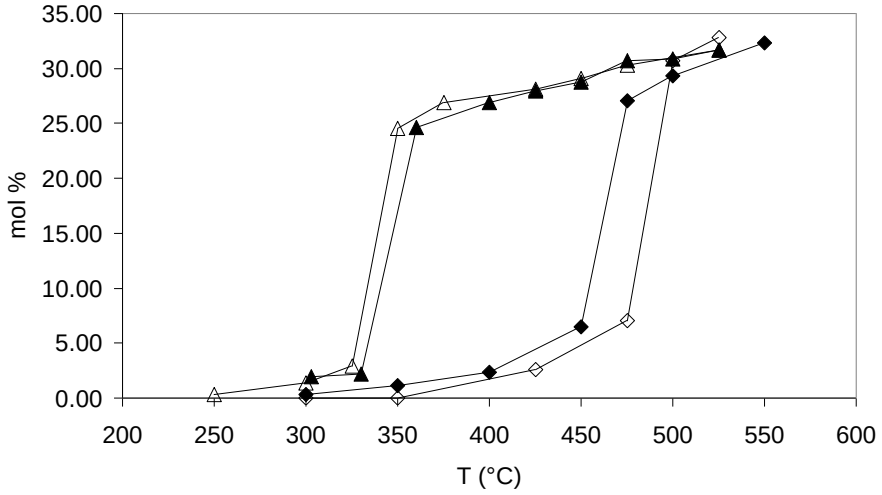

Fig.5

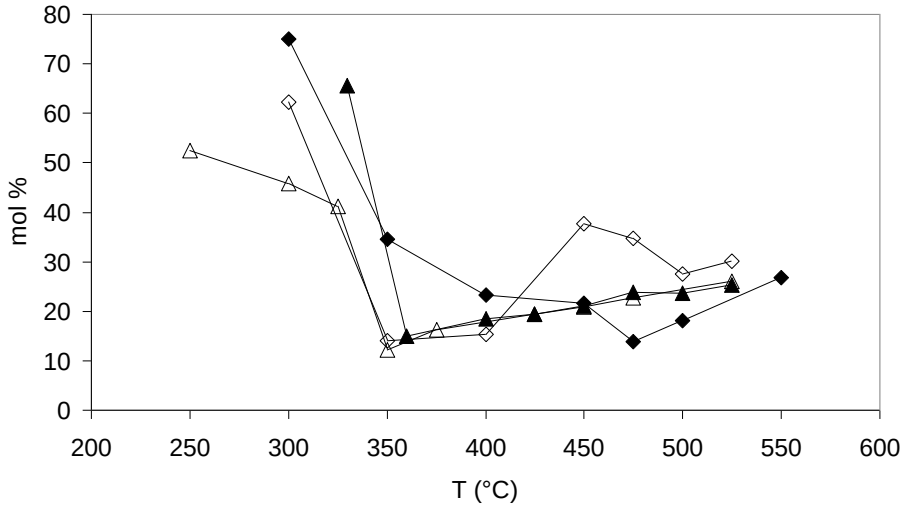

Fig.6

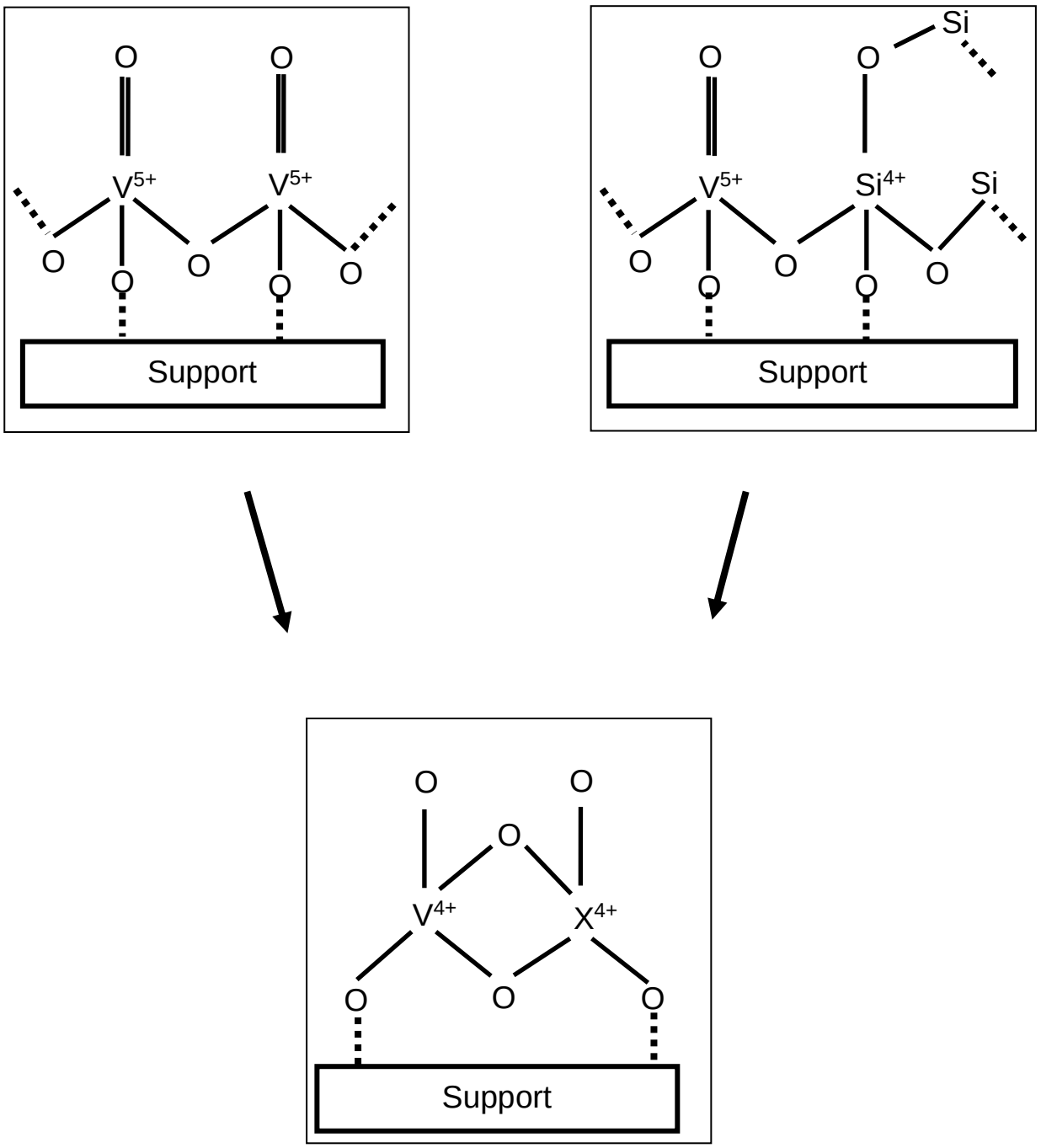
O
O
V5+
V5+
O
O
O
O
O
Support
Si
O
O
V5+
Si4+
Si
O
O
O
O
O
Support
O
O
O
V4+
X4+
O
O
O
Support

Fig. 7

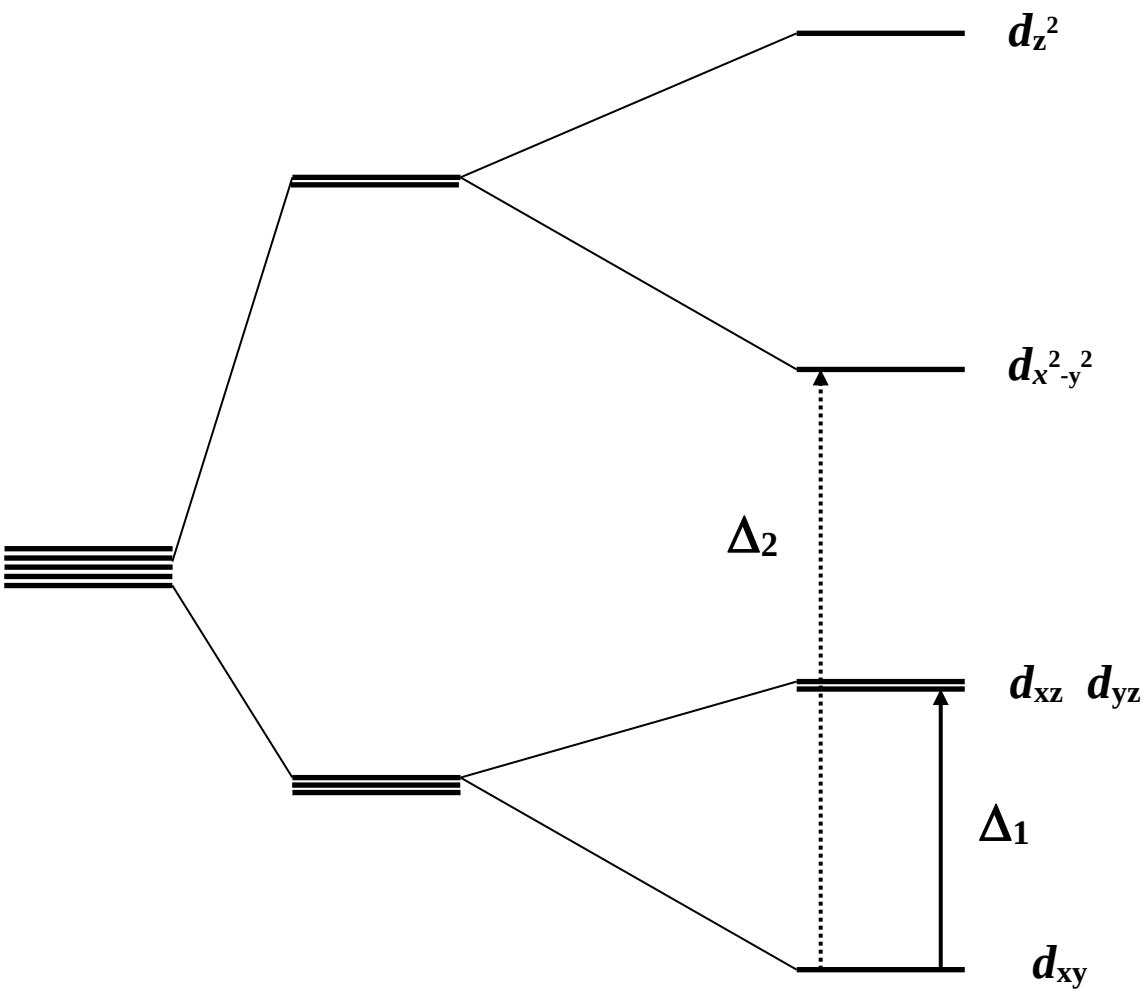

$$g_{//} = g_e - \frac{8\lambda}{\Delta_2}$$

$$g_{\perp} = g_e - \frac{2\lambda}{\Delta_1}$$

Fig.8